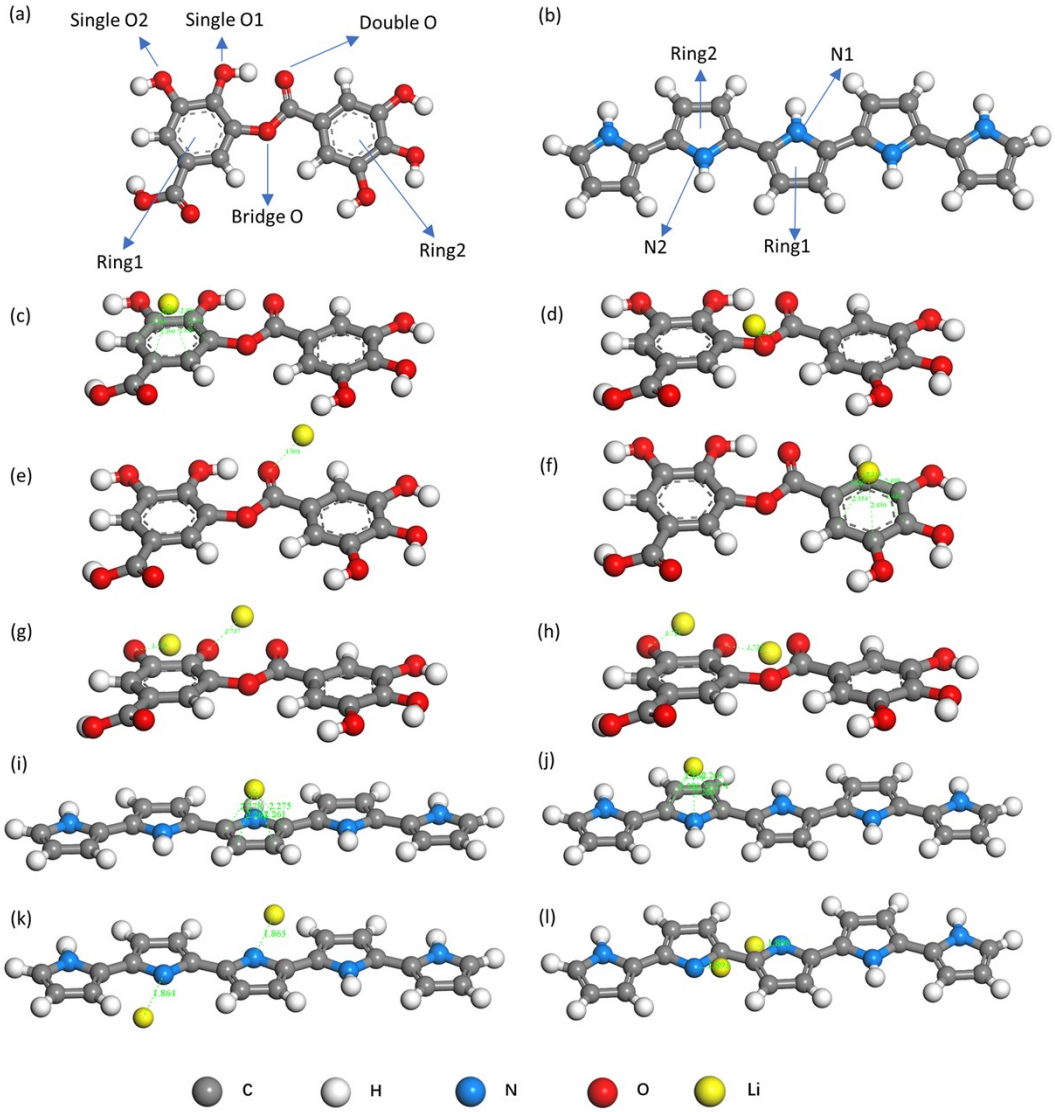

Fig. S1 Schematic diagram of various positions on (a) TA and (b) PPy. The (c) initial and (d) final positions of Li-ion diffusing from ring1 to bridge O above TA. The (e) initial and (f) final positions of Li-ion diffusing from double O to ring2 above TA. The (g) initial and (h) final positions of Li-ion diffusing from single O1 to single O2 above TA. The (i) initial and (j) final positions of Li-ion diffusing from ring1 to ring2 above PPy. The (k) initial and (l) final positions of Li-ion diffusing from N1 to N2 above PPy.

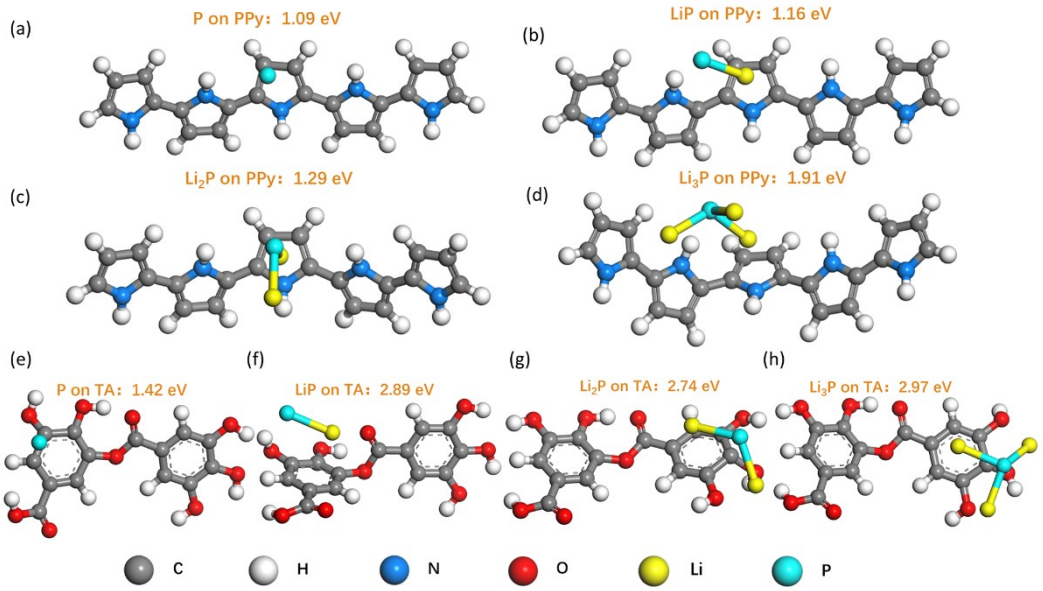

Fig. S2 Adsorption of (a) P, (b) LiP, (c) Li_2P, and (d) Li_3P on PPy.[1] Adsorption of (e) P, (f) LiP, (g) Li_2P, and (h) Li_3P on TA.

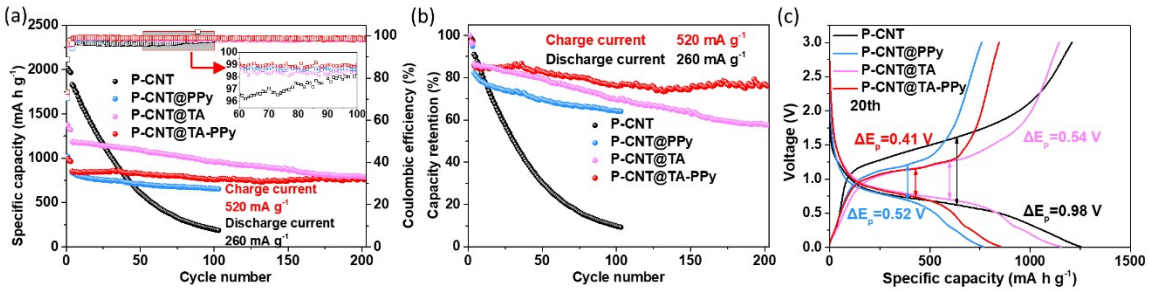

Fig. S3 (a) Cycling performances, (b) capacity retention and (c) the 20th galvanostatic charge/discharge curves of P-CNT, P-CNT@PPy, P-CNT@TA, P-CNT@TA-PPy at 520 mA g^{-1} charge current density and 260 mA g^{-1} discharge current density.

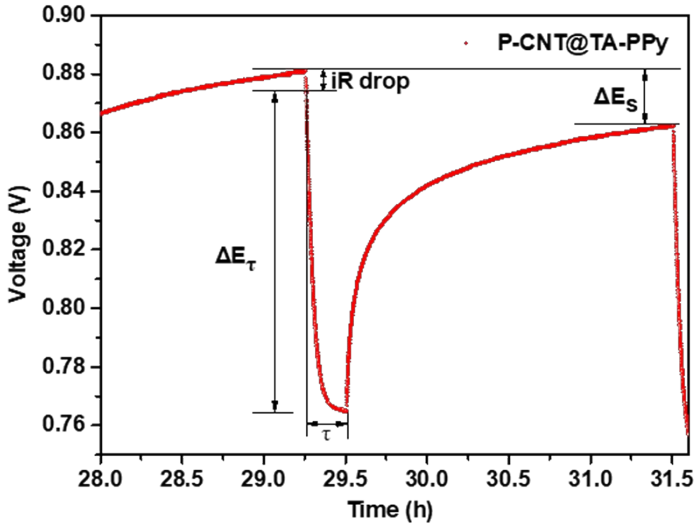

Fig. S4 Schematic labeling of different parameters in GITT.

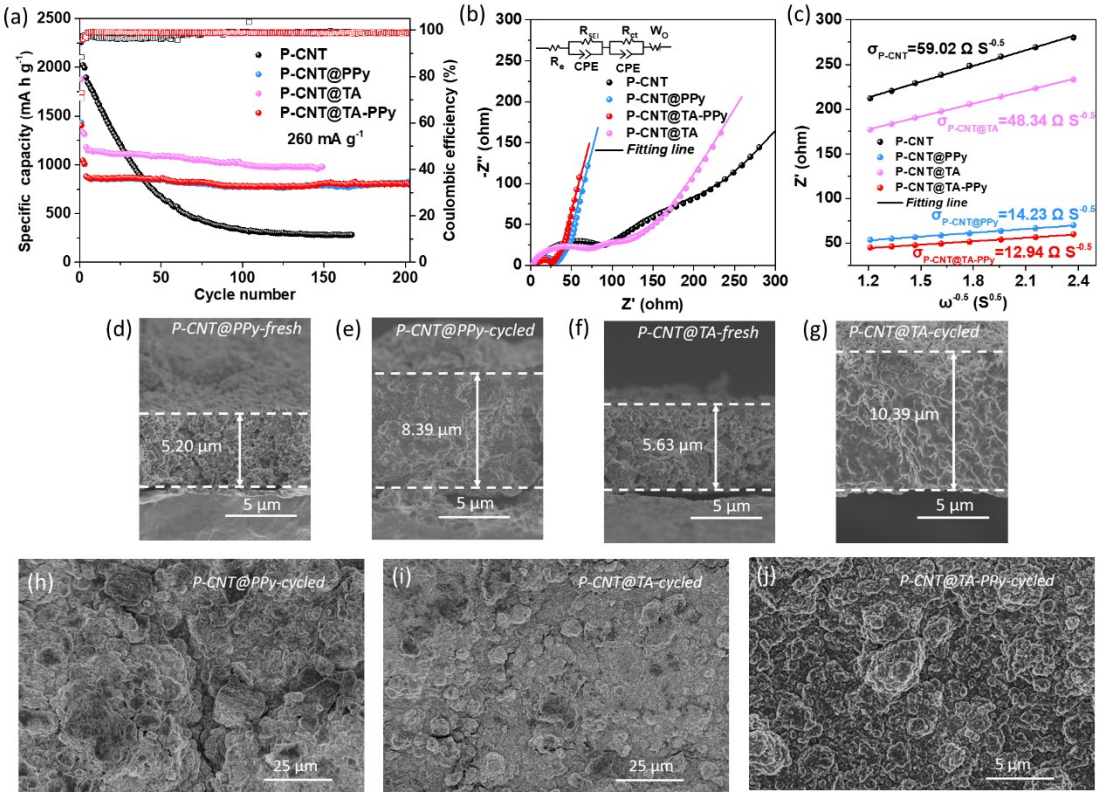

Fig. S5 The dates were tested at both charge and discharge current of 260 mA g^{-1}. (a) Long cycle curves of discharge capacity of P-CNT, P-CNT@PPy, P-CNT@TA, P-CNT@TA-PPy. (b) Nyquist plots of P-CNT, P-CNT@PPy, P-CNT@TA, P-CNT@TA-PPy after 25 cycles and (c) corresponding fitting lines between frequency and Z' in the low frequency region. SEM images showing the thickness and morphology of (d) (e) (h) P-CNT@PPy, (f) (g) (i) P-CNT@TA and (j) P-CNT@TA-PPy electrodes before and after 25 cycles.

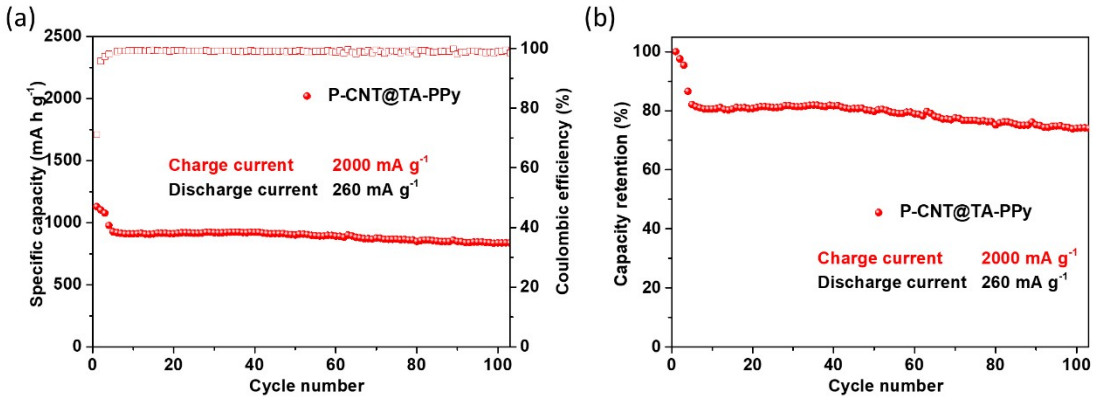

Fig. S6 (a) The cycling performance and (b) corresponding charge capacity retention of P-CNT@TA-PPy at a charge current density of 2000 mA g^{-1} and discharge current density of 260 mA g^{-1}.

Table S1 Cycling performance and multi-rate performance of this work and other works.

Materials	Phosphorus species	Cycling performance	Multi-rate performance	Reference
P-CNT@TA-PPy	Black phosphorus	815 mA h g^{-1} at 260 mA g^{-1}; 757 mA h g^{-1} at 520 mA g^{-1}; 821 mA h g^{-1} at 1000 mA g^{-1}; 837 mA h g^{-1} at 2000 mA g^{-1}	893, 840, 760, 446 mA h g^{-1} at 260, 520, 1300, 5200 mA g^{-1}	This work
P/CNT-10% LiF	Black phosphorus	821 mA h g^{-1} at 50 mA g^{-1}; 783 mA h g^{-1} at 200 mA g^{-1};	1060, 945, 866, 798, 754 and 703 mA h g^{-1} at 25, 50, 100, 200, 500 1000 mA g^{-1}	[S2]
BP/HPC	Black phosphorus	350 mA h g^{-1} at 1000 mA g^{-1};	580, 450, 360, 300, 210 mA h g^{-1} at 50, 200, 500, 1000, 2000 mA g^{-1}	[S3]
BP@CNTs	Black phosphorus	750 mA h g^{-1} at 100 mA g^{-1}; 522 mA h g^{-1} at 500 mA g^{-1};	1450, 950, 800, 550, 420, 380 mA h g^{-1} at 100, 250, 500, 1000, 1500, 2500 mA g^{-1}	[S4]
RP-HC(70%)@TiO_2	Red phosphorus	795 mA h g^{-1} at 100 mA g^{-1}; 447 mA h g^{-1} at 1000 mA g^{-1};	841, 716, 657, 608, 554, 518, 460 mA h g^{-1} at 100, 200, 400, 600, 800,	[S5]

			1000 2000 mA g^{-1}	
BP	Black phosphorus	440 mA h g^{-1} at 740 mA g^{-1};	636, 566, 540, 504, 470, 407 mA h g^{-1} at 460, 1440, 1830, 2750, 3430, 4120 mA h g^{-1}	[S6]
Red phosphorus nanodot/$Ti_3C_2T_x$	Red phosphorus	500 mA h g^{-1} at 50 mA g^{-1}; 818 mA h g^{-1} at 200 mA g^{-1};	599, 434, 347, 260, 197 mA h g^{-1} at 50, 100, 200, 500, 1000 mA g^{-1}	[S7]
BPNs@TiO_2@G	Black phosphorus	502 mA h g^{-1} at 1250 mA g^{-1};	491, 425, 383, 329 mA h g^{-1} at 300, 500, 1000, 2000 mA g^{-1}	[S8]
FP	Fibrous phosphorus	817 mA h g^{-1} at 100 mA g^{-1};	1302, 940, 509, 262, 150 mA h g^{-1} at 100, 200, 500, 1000, 2000 mA g^{-1}	[S9]
TGC-SiC@graphene@P	Fibrous phosphorus	553 mA h g^{-1} at 200 mA g^{-1};	734, 572, 453, 346 mA h g^{-1} at 100, 200, 500, and 1000 mA g^{-1}	[S10]

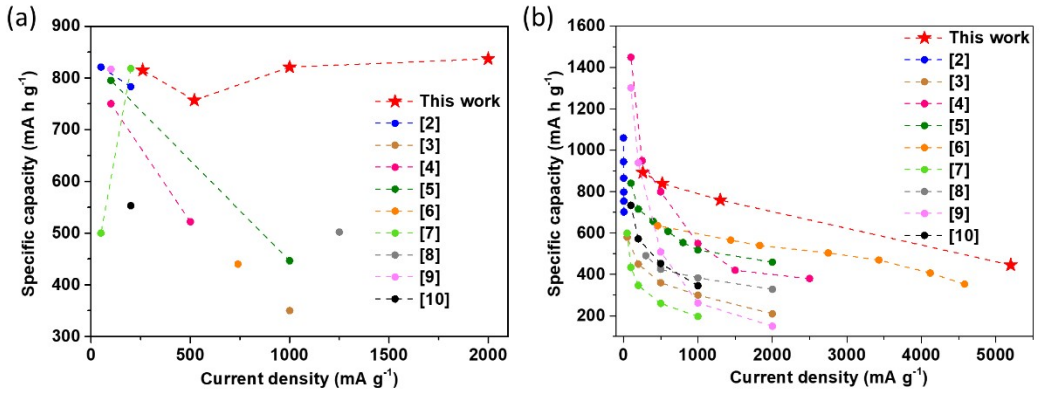

Fig. S7 (a) The cycling performance and (b) multi-rate performance compared with other works.[2-10]

Reference

1 J. Sun, C. Liu, H. Wang, Y. Cao, X. Han, S. Zhang, H. Wang, Y. Zhang, A. Chen, Z. Yang, and J. Sun. *ACS Applied Energy Materials*, 2021, **4**, 4112–4118.

2 C. Liu, M. Han, Y. Cao, L. Chen, W. Ren, G. Zhou, A. Chen, and J. Sun. *Energy Storage Materials*, 2021, **37**, 417–423.

3 S. Zhou, J. Li, L. Fu, J. Zhu, W. Yang, D. Li, and L. Zhou. *ChemElectroChem*, 2020, **7**, 2184–2189.

4 Y. Zhang, L. Wang, H. Xu, J. Cao, D. Chen, and W. Han. *Advanced Functional Materials*, 2020, **30**, 1909372–1909383.

5 D. Wei, Y. Wu, Y. Nie, J. Duan, C. Cao, J. Wu, L. Li, Z. Chen, G. Zhang, and H. Duan. *Applied Surface Science*, 2020, **529**, 147114.

6 Y. Wang, M. He, S. Ma, C. Yang, M. Yu, G. Yin, and P. Zuo. *The journal of physical chemistry letters*, 2020, **11**, 2708–2716.

7 S. Zhang, X. Y. Li, W. Yang, H. Tian, Z. Han, H. Ying, G. Wang, and W. Q. Han. *ACS Applied Materials & Interfaces*, 2019, **11**, 42086–42093.

8 J. Mei, Y. Zhang, T. Liao, X. Peng, G. A. Ayoko, and Z. Sun. *Energy Storage Materials*, 2019, **19**, 424–431.

9 Z. Chen, Y. Zhu, Q. Wang, W. Liu, Y. Cui, X. Tao, and D. Zhang. *Electrochimica Acta*, 2019, **295**, 230–236.

10 D. Zhao, B. Li, J. Zhang, X. Li, D. Xiao, C. Fu, L. Zhang, Z. Li, J. Li, D. Cao, and C. Niu. *Nano Letters*, 2017, **17**, 3376–3382.